

1 Cost-benefit analysis of coastal flood defence measures in the North 2 Adriatic Sea

3 Mattia Amadio¹, Arthur H. Essenfelder¹, Stefano Bagli², Sepehr Marzi¹, Paolo Mazzoli², Jaroslav Mysiak¹,
4 Stephen Roberts³

5 ¹ *Centro Euro-Mediterraneo sui Cambiamenti Climatici, Università Ca' Foscari Venezia, Italy*

6 ² *Gecosistema, Rimini, Italy*

7 ³ *The Australian National University, Canberra, Australia*

8 Abstract

9 The combined effect of [sea level rise](#) and [extreme sea levels](#) and land subsidence phenomena poses a major threat
10 to coastal settlements. Coastal flooding events are expected to grow in frequency and magnitude, increasing
11 the potential economic losses and costs of adaptation. In Italy, a large share of the population and economic
12 activities are located along the coast of the peninsula, although risk of inundation is not uniformly distributed.
13 The low-lying coastal plain of Northeast Italy is the most sensitive to relative sea level changes. Over the last
14 half a century, the entire north-eastern Italian coast has experienced a significant rise in relative sea level, the
15 main component of which was land subsidence. In the forthcoming decades, climate-induced sea level rise is
16 expected to become the first driver of coastal inundation hazard. We propose an assessment of flood hazard
17 and risk linked with extreme sea level scenarios, both under historical conditions and sea level rise projections
18 at 2050 and 2100. We run a hydrodynamic inundation model on two pilot sites located in the North Adriatic
19 Sea along the Emilia-Romagna coast: Rimini and Cesenatico. Here, we compare alternative risk scenarios
20 accounting for the effect of planned and hypothetical seaside renovation projects against the historical
21 baseline. We apply a flood damage model developed for Italy to estimate the potential economic damage
22 linked to flood scenarios and we calculate the change in expected annual damage according to changes in the
23 relative sea level. Finally, damage reduction benefits are evaluated by means of cost-benefit analysis. Results
24 suggest an overall profitability of the investigated projects over time, with increasing benefits due to increased
25 probability of intense flooding in the next future.

26 **Key-words:** coastal inundation Italy extreme sea level rise

27 **Abbreviations:** MSL (Mean Sea Level); TWL (Total Water Level); ESL (Extreme Sea Level); SLR (Sea Level
28 Rise); VLM (Vertical Land Movements); DTM (Digital Terrain Model); EAD (Expected Annual Damage)

29 1. Introduction

30 Globally, more than 700 million people live in low-lying coastal areas (McGranahan et al. 2007), and about
31 13% of them are exposed to a 100-year return period flood event (Muis et al. 2016). On average, one million
32 people located in coastal areas are flooded every year (Hinkel et al. 2014). Coastal flood risk shows an
33 increasing trend in many places due to socio-economic growth (Bouwer 2011; Jongman et al. 2012b) and land
34 subsidence (Syvitski et al. 2009; Nicholls and Cazenave 2010), but in the near future sea level rise (SLR) will
35 likely be the most important driver of increased coastal inundation risk (Hallegatte et al. 2013; Hinkel et al.
36 2014). Evidences show that global sea level has risen at faster rates in the past two centuries compared to the
37 millennial trend (Kemp et al. 2011; Church and White 2011), topping 3.2 mm per year in the last decades
38 mainly due to ocean thermal expansion and glacier melting processes (Mitchum et al. 2010; Meyssignac and
39 Cazenave 2012). According to the IPCC projections, it is very likely that, by the end of the 21st century, the
40 SLR rate will exceed that observed in the period 1971-2010 for all Representative Concentration Pathway (RCP)
41 scenarios (IPCC 2019); yet the local sea level can have a strong regional variability, with some places

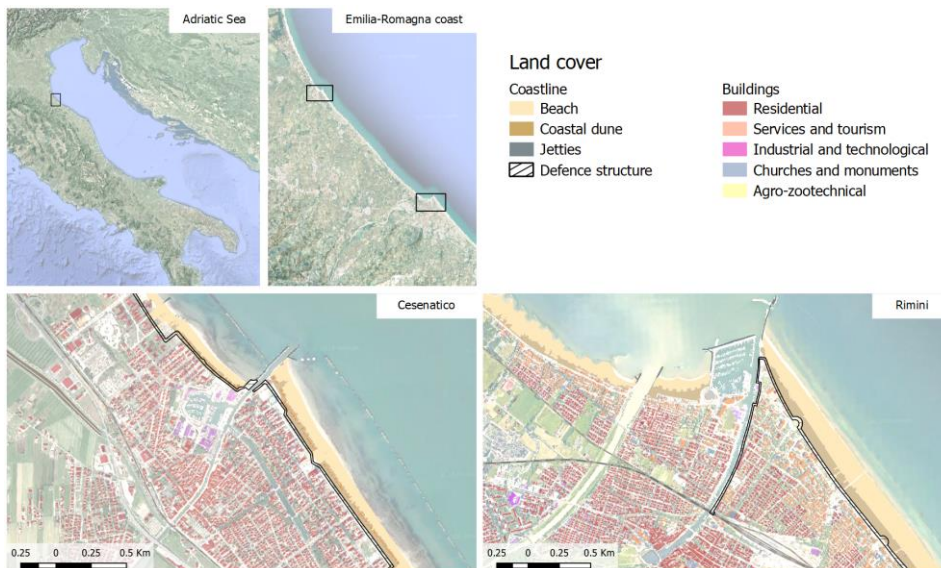
42 experiencing significant deviations from the global mean change (Stocker et al. 2013). This is particularly
43 worrisome in regions where changes in the mean sea level (MSL) are more pronounced, considering that even
44 small increases of MSL can drastically change the frequency of extreme sea level (ESL) events, leading up to
45 situations where a 100-year event may occur several times per year by 2100 (Carbognin et al. 2009, 2010;
46 Vousdoukas et al. 2017, 2018; Kirezci et al. 2020). Changes in the frequency of extreme events are likely to
47 make existing coastal protection inadequate in many places, causing a large part of the European coasts to be
48 exposed to flood hazard. Under these premises, coastal floods threaten to trigger devastating impacts on
49 human settlements and activities (Lowe et al. 2001; McInnes et al. 2003; Vousdoukas et al. 2017). In this context,
50 successful coastal risk mitigation and adaptation actions require accurate and detailed information about the
51 characterisation of coastal flood hazard and the performance of alternative coastal defence options. Cost-
52 benefit analysis (CBA) is widely used to evaluate the economic desirability of a disaster risk reduction (DRR)
53 project (Jonkman et al. 2004; Mechler 2016; Price 2018). CBA helps decision-makers in evaluating the efficacy
54 of different adaptation options (Kind 2014; Bos and Zwaneveld 2017).

55 In this study, ~~designed coastal renovation projects in the municipalities of Rimini and Cesenatico, in Italy, are~~
56 ~~we compared estimate the benefits the effectiveness of of coastal renovation projects along the coast of Emilia-~~
57 ~~Romagna region in (-Italy) -against the baseline scenario- in terms of avoided economic losses net economic~~
58 ~~benefits from ESL inundation events under changing both current and future climate conditions. We select~~
59 ~~two coastal cities along the Emilia Romagna region -as case study areas: i) Rimini, a touristic hotspot in Italy~~
60 ~~that is currently implementing a building a seafront renovation project; and ii) Cesenatico, a coastal city that~~
61 ~~could benefit from similar measures in addition to currently counts existing with a mobile gate system and~~
62 ~~winter sand dunes as coastal flooding defence mechanisms. We design worst-case scenarios of ESL resulting~~
63 ~~from the combination of the maximum levels of mean sea level, vertical land movement, storm surge, tide,~~
64 ~~and wave setup to verify the effectiveness of the above mentioned above-mentioned coastal defence structures~~
65 ~~in reducing flood hazard and related impacts over the urban area under current and future climates. To do~~
66 ~~that. First,~~ we employ the 2D-hydrodynamic ANUGA model (Roberts et al. 2015) for simulating coastal
67 inundation ~~scenarios~~ associated with ESL ~~projections scenarios~~ over the two ~~pilot case study areas~~ located
68 along the Emilia Romagna coast (North Adriatic Sea). ~~The Flood hazard maps scenarios are produced~~
69 ~~calculated for current conditions (2020) and future conditions (2050 and 2100)~~ by combining the
70 ~~local probabilistic~~ data from historical ESL events with the estimates of relative mean sea level (RMSL) change
71 for those locations. RMSL change accounts for both the eustatic global rise and the locally-measured ~~land~~
72 vertical ~~land~~ movement effect. Each inundation scenario simulated by the ~~hydrodynamic~~ model is translated
73 in terms of direct economic impacts over residential areas using a locally-calibrated damage model. The
74 combination of different risk scenarios in a CBA framework allows to evaluate the economic benefits brought
75 by the project implementation in terms of avoided direct flood losses up to the end of the century.

76 2. Area of study

77 Located in the central Mediterranean Sea, the Italian peninsula has more than 8,300 km of coasts, hosting
78 around 18% of the country population, numerous towns and cities, industrial plants, commercial harbours
79 and touristic activities, as well as cultural and natural heritage sites. Existing country-scale estimates of SLR
80 ~~impacts~~ up to the end of this century helps to identify the most critically exposed coastal areas of Italy
81 (Lambeck et al. 2011; Bonaduce et al. 2016; Antonioli et al. 2017; Marsico et al. 2017). About 40% of the ~~country's~~
82 coastal perimeter consist of a flat coastal profile (ISPRA 2012), potentially more vulnerable to the impacts of
83 ESL events. The North Adriatic coastal plain is acknowledged to be the largest and most vulnerable location
84 to extreme coastal events due to the shape, morphology and low bathymetry of the Adriatic sea basin, which

85 cause water level to increase relatively fast during coastal storms (Carbognin et al. 2010; Ciavola and Coco
 86 2017; Perini et al. 2017). The ESL here is driven mainly by astronomical tide, ranging about one meter in the
 87 northernmost sector; and meteorological forcing, such as low pressure, seiches and prolonged rotational wind
 88 systems, which are the main trigger of storm surge in the Adriatic basin (Vousdoukas et al. 2017; Umgiesser
 89 et al. 2020). In addition to that, all the coastal profile of the Padan plain shows relatively fast subsiding rates,
 90 partially due to natural phenomena, but in large part linked to human activities (Carbognin et al. 2009; Perini
 91 et al. 2017; Meli et al. 2021). As a contributing factor to coastal flood risk, the intensification of urbanization
 92 has led to increased exposure along the Adriatic coast during the last 50 years, with many regions building
 93 over half of the available land within 300 meters from the shoreline (ISPRA 2012). This study focuses on two
 94 pilot sites located along the Adriatic coast of Emilia Romagna, shown in Figure 1 shows the location of the
 95 two case study areas, -Cesenatico and Rimini, along with land-cover maps showing the position of coastal
 96 defences accounted in this study.-



97
 98 **Figure 1. Pilot areas Case-study** locations along the Emilia-Romagna coast: Cesenatico and Rimini. The coastal
 99 defence structure assessed in this study are shown in black. Buildings' footprint data from Regional
 100 Environmental Agency (ARPA) 2020. Basemap © Google Maps 2020.

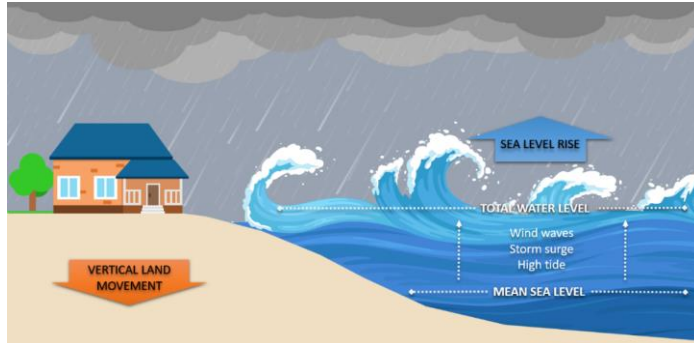
101 The number of ESL events reported to cause impacts along the Emilia-Romagna coast shows a steady increase
 102 since the second half of the past century (Perini et al. 2011), which is in part explained by to the socio-economic
 103 development of the coast exposing increasing asset to flood risk. The landscape along the 130 km regional
 104 coastline is almost flat, the only relief being old beach ridges, artificial embankments and a small number of
 105 dunes. The coastal perimeter is delineated by a wide sandy beach that is generally protected by offshore
 106 breakwaters, groins and jetties. The land elevation is often close to (or even below) the MSL, while the coastal
 107 corridor is heavily urbanised. Cesenatico has about 26,000 residents, while Rimini has 150,000. These-The
 108 towns port towns have a strong touristic vocation, hosting large beach resort and bathing facilities along the
 109 beach and hundreds of hotels and rental housing located just behind the seaside. Both towns-places have been
 110 affected by coastal storms resulting in flooding of buildings and activities, beach erosion and regression of the
 111 coastline. The most recent inundation events were observed in March 2010, November 2012 and February

112 2015. The 2015 event was one of the most severe ever recorded, with ESL values corresponding to a probability
113 of once in 100 years. It caused severe damages along the whole regional coast and, in some locations, required
114 the evacuation of people from their houses; many buildings and roads were covered by sand brought by the
115 flood wave; touristic infrastructures near the shore were seriously damaged, and some port channels
116 overflowed the surrounding areas. The economic impact of the event was estimated topping 7.5 M Eur (Perini
117 et al. 2015).

118 3. Methodology

119 3.1 Components of the analysis

120 Coastal inundation phenomena are caused by an increase of total water level (TWL), most often associated
121 to extreme sea level (ESL) events, which are often generated by a combination of high astronomical tide and
122 meteorological drivers such as storm surge and wind waves (figure 2). Estimates of ESL are obtained for the
123 North Adriatic up to year 2100 by combining reference hazard scenarios derived from historical records with
124 regionalised projections of SLR (Vousdoukas et al. 2017) and local vertical land movements (VLM) rates
125 (Carbognin et al. 2009; Perini et al. 2017). Four ESL frequency scenarios, namely once in 1, 10, 100- and 250-
126 years, are considered. The hydrodynamic model ANUGA is applied to simulate the inundation of land areas
127 during ESL accounting for individual components (storm surge, tides and waves). Land morphology and
128 exposure of coastal settlements are described by high-resolution DTM and bathymetry, in combination with
129 land use and buildings footprints. The effect of hazard mitigation structures (both designed and under
130 construction) are explicitly accounted in the “defended” simulation scenario, in contrast to the baseline
131 scenario, where only existing defence structures (groins, jetties, breakwaters and sand dunes) are accounted.



132
133 **Figure 2.** Components of the analysis for extreme sea level events: total water level is the sum of maximum
134 tide, storm surge and wind waves over mean sea level. Vertical land movement and eustatic sea level rise
135 affects the mean sea level on the long run.

136 3.2 Vertical Land Movement

137 Vertical land movements result from a combination of slow geological processes such as tectonic activity and
138 glacial isostatic adjustment (Peltier 2004; Peltier et al. 2015), and medium-term phenomena, such as sediment
139 loading and soil compaction (Carminati and Martinelli 2002; Lambeck and Purcell 2005). The latter can greatly
140 oversize geological processes at local scale (Wöppelmann and Marcos 2012); in particular, faster subsidence
141 occurs in presence of intense anthropogenic activities such as water withdrawal and natural gas extraction
142 (Teatini et al. 2006; Polcari et al. 2018). Most of the peninsula shows a slow subsiding trend, although with

143 some local variability. An estimate of VLM rates due to tectonic activity has been derived from studies
144 conducted in Italy (Lambeck et al. 2011; Antonioli et al. 2017; Marsico et al. 2017; Solari et al. 2018). The North
145 Adriatic coastal plain shows the most intense long-term geological subsidence rates (about 1 mm per year),
146 increasing North to South. Yet in the last decades these rates were often greatly exceeded by ground
147 compaction rates observed by multi-temporal SAR Interferometry (Gambolati et al. 1998; Antonioli et al. 2017;
148 Polcari et al. 2018; Solari et al. 2018). Observed subsidence is about one order of magnitude faster where the
149 aquifer system has been extensively exploited for agricultural, industrial and civil use since the post-war
150 industrial boom. From the 1970s, however, with the halt of groundwater withdrawals, anthropogenic drivers
151 of subsidence has been strongly reduced or stopped, but many of the induced effects still remain (Carbognin
152 et al. 2009). Nonetheless, subsidence still continues at rates much larger faster rates than the natural
153 one expected from natural phenomena on areas a few kilometres inland from the coastal line, at rates of about
154 10 mm/yr (Teatini et al., 2005) (Teatini et al. 2005). Geodetic surveys carried out from 1953 to 2003 along the
155 Ravenna coast provide evidence of a cumulative land subsidence exceeding 1 m at some sites due to gas
156 extraction activities. Average subsidence rates observed for 2006-2011 along the Emilia-Romagna coast are
157 around 5 mm/yr, exceeding 10 mm/yr in the back shore of the Cesenatico and Rimini areas and topping 20-50
158 mm/yr in Ravenna (Carbognin et al. 2009; Perini et al. 2017). Based on these current rates, we assume an
159 average fixed annual VLM of 5 mm in both Cesenatico and Rimini up to the end of the century. This
160 remarkable difference between natural VLM rates and observations would produce a dramatic effect on the
161 estimated SLR scenarios: at present rates, Rimini would see an increase of MSL by 0.15 m in 2050 and more
162 than 0.4 m in 2100 independently from eustatic SLR. Since these rates are connected with human activity, it is
163 not possible to foresee exactly how they will change in the long term.

164 3.3 Sea Level Rise

165 The long availability of tide gauge data along the North Adriatic coast allows to assess the changes in MSL
166 during the last century. Records from the gauge station of Marina di Ravenna show an eustatic rise of 1.2 mm
167 per year from 1890 to 2007 (Meli et al. 2021), in good agreement with the eustatic rise measured at other stations
168 in the Mediterranean Sea (Tsimplis and Rixen 2002; Carbognin et al. 2009). The projections of future MSL
169 account for sea thermal expansions from four global circulation models, estimated contributions from ice-
170 sheets and glaciers (Hinkel et al. 2014) and long-term subsidence projections (Peltier 2004). The ensemble mean
171 is chosen to represent each RCP for different time slices. The increase in the central Mediterranean basin is
172 projected to be approximately 0.2 m by 2050 and between 0.5 and 0.7 m by 2100, compared to historical mean
173 (1970-2004) (Vousdoukas et al. 2017). As agreed with stakeholders, our analysis considers the intermediate
174 emission scenario RCP 4.5, projecting an increase in MSL of 0.53 m at 2100. It must be noted that these
175 projections, although downscaled for the Adriatic basin, do not account for the peculiar continental
176 characteristics of the shallow northern Adriatic sector, where the hydrodynamics and oceanographic
177 parameters partially depend on the freshwater inflow (Zanchettin et al. 2007).

178 3.4 Tides and meteorological forcing

179 Storm surge and wind waves represent the largest contribution to TWL during an ESL event. An estimation
180 of these components is obtained for the pilot two coastal sites from the analysis of tide gauge and buoy
181 records, and from the description of historical extreme events presented in local studies (Perini et al. 2011,
182 2012, 2017; Masina et al. 2015; Armaroli and Duo 2018). This area is microtidal: the mean neap tidal range is
183 30–40 cm, and the mean spring tidal range is 80–90 cm. Most storms have a duration of less than 24 h and a
184 maximum significant wave height of about 2.5 m. During extreme cyclonic events, the sequence of SE wind
185 (*Sirocco*) piling the water North and E-NE wind (*Bora*) pushing waves towards the coast can generate severe

186 inundation events, with significant wave height ranging 3.3 – 4.7 m and exceptionally exceeding 5.5 m
187 (Armaroli et al. 2012). Fifty significant events have been recorded from 1946 to 2010 on the ER coast, with half
188 of them causing severe impacts along the whole coast and 10 of them being associated with important flooding
189 events (Perini et al. 2017). The most severe events are found when strong winds blow during exceptional tide
190 peaks, most often happening in late autumn and winter. The event of November 1966 represents the highest
191 ESL on records, causing significant impacts along the regional coast: the recorded water level was 1.20 m above
192 MSL, and wave heights offshore were estimated around 6–7 m (Perini et al. 2011; Garnier et al. 2018). The
193 whole coastline suffered from erosion and inundation, especially in the province of Rimini. Atmospheric
194 forcing shown significant variability for the period 1960 onwards (Tsimplis et al. 2012), but there is no strong
195 evidence supporting a significant change in trend for the next future (Lionello 2012; Lionello et al. 2020;
196 Zanchettin et al. 2020). Thus, we assume the frequency and intensity of meteorological events to remain the
197 same up to 2100.

198 3.5 Terrain morphology and coastal defence structures

199 Reliable bathymetries and topography are required in order to run the hydrodynamic modelling at the local
200 scale. Bathymetric data for the Mediterranean Sea were obtained from the European Marine Observation and
201 Data Network (EMODnet) at 100 m resolution. The description of terrain morphology comes from the official
202 high-resolution LIDAR DTM (MATTM, 2019). First, we combined the coastal dataset (2 m resolution and
203 vertical accuracy of ± 0.2 m), and the inland dataset (1 m resolution and vertical accuracy ± 0.1 m) into one
204 seamless layer. Then, the DTM is supplemented with geometries of existing coastal protection elements such
205 as jetties, groins and breakwaters obtained from the digital Regional Technical Map. In Rimini, the *Parco del*
206 *Mare* (figure 3) is an urban renovation project which aims to improve the seafront promenade: the existing
207 road and parking lots are converted into an urban green infrastructure consisting of a concrete barrier covered
208 by vegetated sandy dunes with walking paths. This project also acts as a coastal defence system during
209 extreme sea level events. The barrier rises 2.8 meters along the southern section of the town, south of the
210 marina; no barrier is planned on the northern coastal perimeter. The *Parco del Mare* project ~~is~~, currently under
211 construction ~~and~~ has been taken in account in the evaluation of the “defended” scenarios by ~~merging adding~~
212 the barrier ~~into~~ the existing DTM (figure 3).

Formatted: Font: Italic

Formatted: Font: Palatino Linotype, 10 pt, Italic



213
214 **Figure 3.** Prototype design of Parco del Mare project in Rimini. Adapted from JDS Architects.

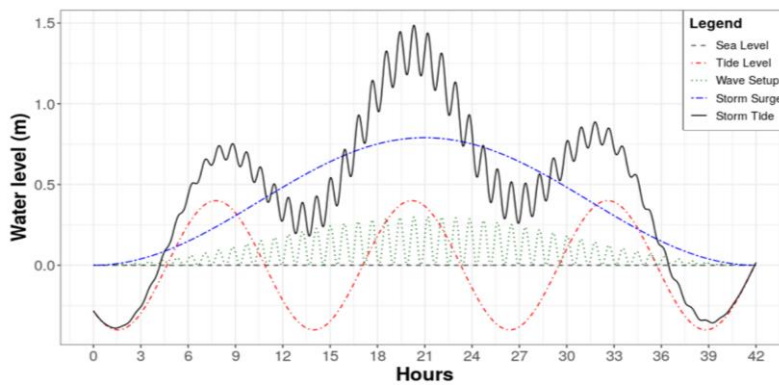
215 In Cesenatico, the existing defence structures include a moving barrier~~s~~ system (*Porte Vinciane*) located on the
216 port channel, coupled with a dewatering pump which discharge the meteoric waters in the sea. The barriers
217 close automatically if the TWL surpasses 1 meter over the mean sea level, preventing floods in the historical
218 centre up to ESL of 2.2 meters of TWL. Additional defence structures include the winter dunes, which consist
219 of a 2.2 meter-tall intermittent, non-reinforced sand barrier. In the defended scenario, we envisage a coastal
220 defence structure similar to Rimini's Parco del Mare project in Rimini, spanning both North and South of the

Formatted: Font: Palatino Linotype, 10 pt, Italic

221 port channel with a total length of 7.8 km. A proper setup of the inundation model required to first perform
222 some manual editing of the DTM using additional reference data (i.e. on-site observations or aerial
223 photography) in order to produce an elevation model that realistically represent the land morphology and
224 associated water dynamics (e.g. removal of non-existent sink holes). Bridges and tunnels are the most critical
225 elements that required DTM correction in order to avoid misrepresentations of the water flow routing.

226 3.6 Inundation modelling

227 At the local scale, hydrodynamic models represent an efficient compromise between hydrostatic and hydraulic
228 models, being able to perform realistic simulations of inundation phenomena and to obtain detailed
229 information about the hazard features, while requiring a relatively fast setup and reasonable computational
230 effort. In this study we use ANUGA, a 2D hydrodynamic model originally developed to simulate tsunami
231 events, which is also suitable for the simulation of hydrologic phenomena such as riverine peak flows and
232 storm surges (Roberts 2020). Being a 2D hydrodynamic model, ANUGA does not resolve vertical convection
233 ~~and consequently, not breaking~~ waves ~~breaking~~ or 3D turbulence (e.g. vorticity), thus ~~it does not not~~
234 ~~considering account for~~ the swash component of wave runup. The fluid dynamics in ANUGA is based on a
235 finite-volume method for solving the shallow water wave equations, thus being based on continuity and
236 simplified momentum equation. The model computes the total water level, the water depth, and the horizontal
237 momentum on an irregular triangular grid based on the provided forcing conditions. ANUGA includes also
238 an operator module that simulates the removal of sand associated with over-topping of a sand dune by sea
239 waves, which is applied to explore scenarios where a sand dune barrier provides protection for the land
240 behind. The operator simulates the erosion, collapse, fluidisation and removal of sand from the dune system
241 (Kain et al. 2020); the dune erosion mechanism relies on a relationship based on Froehlich (2002). This option
242 is enabled only in the undefended scenario for Cesenatico, where non-reinforced sand dunes are prone to
243 erosion.



244
245 **Figure 4.** Total Water Level (black) as a sum of tide (red), storm surge (blue) and wave setup (green) for ESL
246 scenario 1 in 10 years.

247 In our application, we estimate the TWL on the coastland at every timestep as the sum of extreme values for
248 storm surge level (SS), wave setup (Ws), and max tide (T_{max}), as shown in figure 4. Storm surge peak is set to
249 coincide with the tidal peak at in the mid of the event, thus producing a maximum TWL value. As considered,
250 our approach is precautionary as it provides worst-case scenario ESL values. We draw theseThe components
251 of TWL are obtained variables from the existing probabilistic analysis of extreme events conducted on the
252 regional coast (Perini et al. 2016, 2017) and later adopted by the Regional Environmental Agency to define the

253 official coastal flood hazard zones (ARPAE 2019). The probability of occurrence for ESL scenarios is expressed
 254 in terms of return period (RP), which is the estimated average time interval between events of similar intensity,
 255 accounting for all variables combined. The maximum tidal excursion is 0.8-0.9 m, while wave height can range
 256 from 3 to almost 6 m during strong wind events, translated into a wave setup near the shore can range ranging
 257 from 0.22 to 0.65 m. For RP 250, TWL reaches hits 2.5 meters yet as all components reach their most extreme
 258 values T_{max} is not explicitly available, being hence estimated as the difference from TWL and the other
 259 components. Additional details are wave period (Wp , in seconds) and event duration ($Time$, in hours), required
 260 for the hydrodynamic simulation of coastal flooding to events and the determination of the estimate the
 261 maximum extent of inland water propagation. We obtain Wp . Both variables are obtained from existing
 262 analysis of historical ESL events records, matched with the probabilistic distribution of RP scenarios (Armaroli
 263 et al. 2012; Armaroli and Duo 2018). In our scenarios, Wp wave direction is set to be oriented perpendicular to
 264 the coast. Storm surge is set to peak in the mid of the event, producing the maximum TWL value for the
 265 event. Table 1 summarizes the ESL components according to the four probability scenarios identified from local
 266 historical records (Perini et al. 2017). The probability of occurrence is expressed in terms of return period (RP),
 267 which is the estimated average time interval between events of similar intensity. The output of the simulation
 268 consists of maps representing flood extent, water depth and momentum at every time step (1 second),
 269 projected on the high-resolution DTM grid.

270 **Table 1.** components of TWL during an ESL event under historical conditions and projected conditions (2050
 271 and 2100), accounting for both eustatic SLR (RCP 4.5) and average VLM rate.

RP (years)	Extreme event features				Historical	2050			2100		
	SS (m)	T_{max} (m)	W_s (m)	$Time$ (h)	TWL (m)	SLR (m)	VLM (m)	TWL (m)	SLR (m)	VLM (m)	TWL (m)
1	0.60	0.40	0.22	32	1.2	0.14	0.19	1.55	0.53	0.44	2.2
10	0.79	0.40	0.30	42	1.5	0.14	0.19	1.82	0.53	0.44	2.5
100	1.02	0.40	0.39	55	1.8	0.14	0.19	2.14	0.53	0.44	2.8
250	1.40	0.45	0.65	75	2.5	0.14	0.19	2.83	0.53	0.44	3.5

272 3.7 Risk modelling and Expected Annual Damage

273 Direct damage to physical asset is estimated using a customary flood risk assessment approach originally
 274 developed for fluvial inundation, which is adapted to coastal flooding assuming that the dynamic of impact
 275 from long-setting floods depends on the same factors, namely: 1) hazard magnitude, and 2) size and value of
 276 exposed asset. Indirect economic losses due to secondary effects of damage (e.g. business interruption) are
 277 excluded from the computation. Hazard magnitude can be defined by a range of variables, but the most
 278 important predictors of damage are water depth and the extension of the flood event (Jongman et al. 2012a;
 279 Huizinga et al. 2017). Land cover definitions and buildings footprints help to estimate the exposed capital
 280 including residential buildings, commercial and industrial activities, infrastructures, historical and natural
 281 sites. The characterization of exposed asset is built from a variety of sources, starting from land use and
 282 buildings footprints obtained from the Regional Environmental Agencies geodatabases and the Open Street
 283 Map database (Geofabrik GmbH 2018). Additional indicators about buildings characteristics are obtained
 284 from the database of the official-2016 Italian Census of 2011 (ISTAT 2011), while mean construction and
 285 restoration costs per building types are obtained from cadastral estimates (CRESME 2014). The asset
 286 representation is static, thus not accounting for changes in land use nor population density, while allowing for
 287 the direct comparison of hazard mitigation options' results. A depth-damage function was previously
 288 validated on empirical records (Amadio et al. 2019) and then applied in order to translate each hazard scenario
 289 into an estimate of economic risk, measured as a share of total exposed value. The damage function applies

Field Code Changed

Formatted: English (United States)

Formatted: English (United States)

Formatted: Font: Palatino Linotype, 10 pt, English (United States)

290 only to residential and mixed-residential buildings, the area of which represents about 93% of total exposed
 291 footprints; other types (such as harbour infrastructures, industrial, commercial, historical monuments and
 292 natural sites) are excluded from risk computation. Abandoned or under-construction buildings are also
 293 excluded from the analysis. To avoid overcounting of marginally-affected buildings, we set two threshold
 294 conditions for damage calculation: flood extent must be greater than or equal to 10 m², and maximum water
 295 depth greater than or equal to 10 cm. The damage/probability scenarios are combined together as Expected
 296 Annual Damage (EAD). EAD is the damage that would occur in any given year if damages from all flood
 297 probabilities were spread out evenly over time; mathematically, EAD is the integration of the flood risk density
 298 curve over all probabilities (Olsen et al. 2015), as in equation 1.

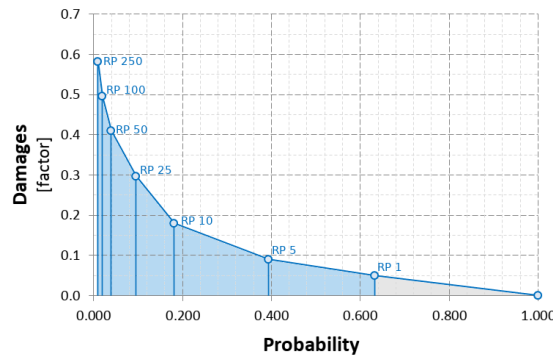
$$EAD = \int_0^1 D(p) dp \quad (1)$$

299 The integration of the curve can be solved either analytically or numerically, depending on the complexity of
 300 the damage function $D(p)$. Several different methods for numerical integration exist; we use an approach
 301 where EAD is the sum of the product of the fractions of exceedance probabilities by their corresponding
 302 damages (figure 5). We calculate $D(p)$, which is the damage that occurs at the event with probability p , by
 303 using the depth-damage function for each hazard scenario. The exceedance probability of each event (p) is
 304 calculated based on exponential function as shown in equation 2.

$$p = 1 - e^{\left(\frac{-1}{RP}\right)} \quad (2)$$

305 Events with a high probability of occurrence and low intensity (below RP 1 year) are not simulated, as they
 306 are assumed to not cause significant damage. This is consistent with the historical observations for the case
 307 study area, although this assumption could change with increasing MSL.

Figure 5. Schematic representation of the numerical integration of the damage function $D(p)$ with respect to the exponential probability of the hazard events. Events with a probability of occurrence higher than once in a year are expected to not cause damage (grey area).



308 3.8 Cost-Benefit Analysis

309 A CBA should include a complete assessment of the impacts brought by the implementation of the hazard
 310 mitigation option, i.e. direct and indirect, tangible and intangible impacts (Bos and Zwaneveld 2017). The
 311 project we are considering, however, has not been primarily designed for DRR purpose: instead, it is meant
 312 as an urban renovation project which aims to consolidate the touristic vocation of the area, to improve the
 313 quality of life and the urban environment (Comune di Rimini 2018). This implies some large indirect effects
 314 on the whole area, most of which are not strictly related to disaster risk management and, overall, very difficult
 315 to estimate ex-ante. Our evaluation focuses only on the benefits that are measurable in terms of direct flood
 316 losses reduction. Regarding the implementation costs, the CBA accounts for the initial investment required

317 for setting up the adaptation measure, and operational costs through time. According to the *“Parco del Mare.”*
 318 project funding documentation (Comune di Rimini 2019a, b, 2020, 2021a, b), the total cost of the project (to be
 319 completed during 2021) is 33.3 M Eur, corresponding to 5.55 M Eur per Km of length. No information is
 320 available about maintenance costs of the opera, but given the nature of the project (static defense with low
 321 structural fragility), we assume they will be rather small compared to the initial investment. Ordinary annual
 322 maintenance costs are accounted as 0.1% of the total cost of the project. The same costs are assumed for the
 323 hypothetical barrier in Cesenatico, resulting in an initial investment cost of 43.3 M. Costs and benefit occurring
 324 in the future periods need to be discounted, as people put higher value on the present (Rose et al., 2007). This
 325 is done by adjusting future costs and benefits using an annual discount rate (r). We chose a variable rate of $r =$
 326 3.5 for the first 50 years and $r = 3$ from 2050 onward (Lowe 2008). A sensitivity analysis of discount rate is
 327 included in Annex 1. The three main decision criteria used in CBA for project evaluation are the Net Present
 328 Value (NPV), the Benefit/Cost Ratio (BCR) and the payback period. The NPV is the sum of Expected Annual
 329 Benefits (B) up to the end of the time horizon, discounted, minus the total costs for the implementation of the
 330 defense measure, which takes into account initial investment plus discounted annual maintenance costs (C).
 331 In other words, the NPV of a project equals the present value of the net benefits ($NB_t = B_t - C_t$) over a period of
 332 time (Boardman et al. 2018), as in equation (3):

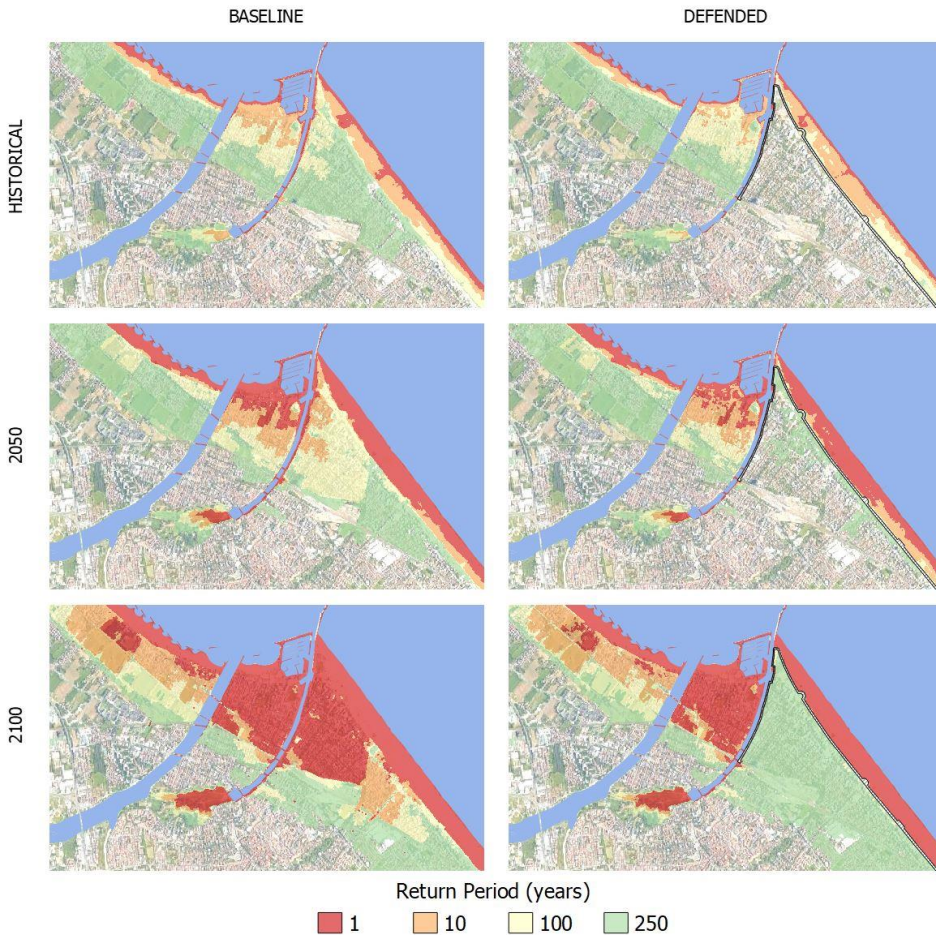
$$NPV = PV(B) - PV(C) = \sum_{t=0}^n \frac{NB_t}{(1+r)^t} \quad (3)$$

333 Positive NPV means that the project is economically profitable. The BCR is instead the ratio between the
 334 benefits and the costs; a BCR larger than 1 means that the benefits of the project exceed the costs on the long
 335 term and the project is considered profitable. The payback period is the number of years required for the
 336 discounted benefits to equal the total costs.

337 4. Results

338 4.1 Inundation scenarios

339 Once the setup is completed, the hydrodynamic model performs relatively fast: each simulation is carried at
 340 half speed compared to real time, requiring about 24 hours to simulate a 12 h event. Parallel simulations for
 341 the same area can run on a multicore processor, improving the efficiency of the process. The output of the
 342 hydrodynamic model consists of a set of inundation simulations that include several hazard intensity variables
 343 in relation to flood extent: water depth, flow velocity, and duration of submersion. ESL scenarios are then
 344 summarized into static maps, each one representing the maximum value reached by hazard intensity variables
 345 ~~during the simulated event at grid cell level (about 1 meter resolution) during the whole simulated event.~~ The
 346 flood extents corresponding to each RP scenario are shown for Rimini (figure 6) and Cesenatico (figure 7).

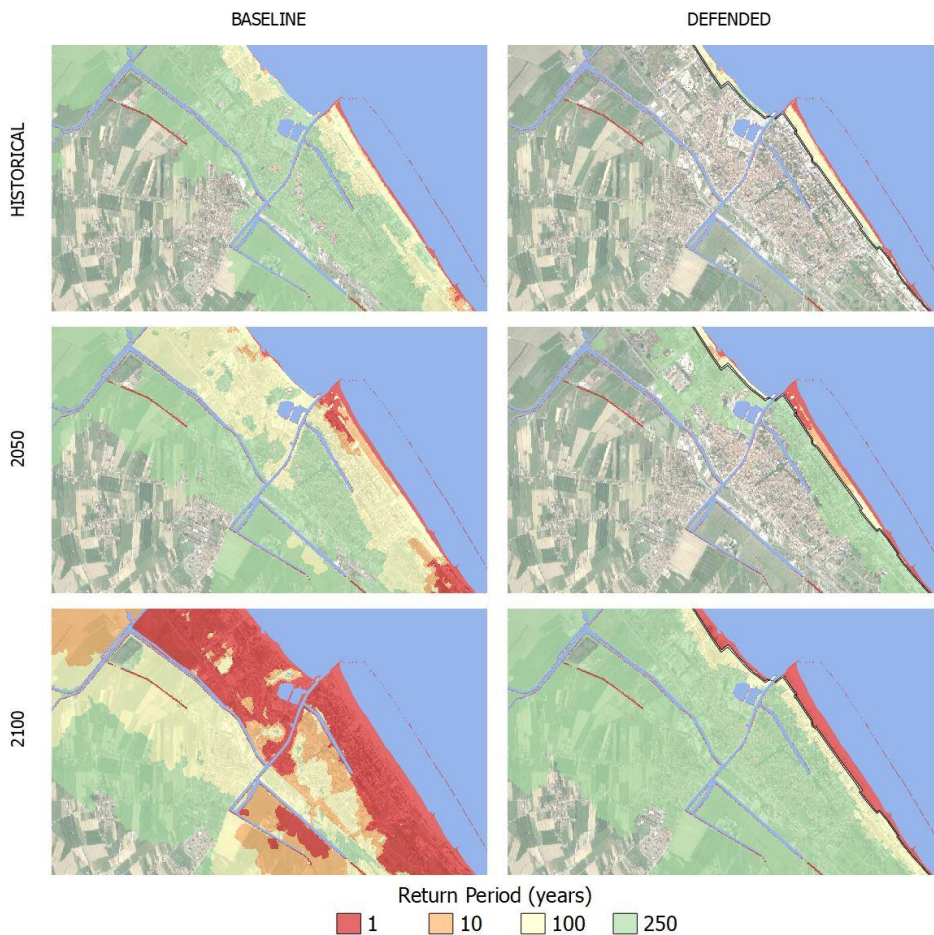


347

348 **Figure 6.** Rimini, extent of land affected by flood according to frequency of occurrence of ESL event up to 2100
 349 for the baseline [left] and the defended scenario [right]. Basemap © Google Maps 2020.

350 In Rimini, the *Parco del Mare* barrier produces benefits in terms of avoided damage in the south-eastern part
 351 of the town (high-density area) for ESL events with a return period of 100 years or less. The north-western part
 352 of the town and the marina are outside of the defended area; these areas are therefore subject to a similar amount of
 353 flooding across scenarios. In all the simulations, the buildings located behind the marina are the firsts to be
 354 flooded. In fact, the new and the old port channels located on both sides of the marina represent a hazard
 355 hotspot: as shown in the maps, the failure of the eastern channel, which has a relatively low elevation, is likely
 356 to cause the water to flood the eastern part of the town, even during inundation events that would not surpass
 357 the beach. In the defended scenarios, where both the coastal and the canal barriers are enabled, the flood extent
 358 in the ~~SE-south-eastern~~ urban area becomes almost zero for ESL events with a probability of once in 100 years,
 359 even when accounting for SLR up to 2100. Under ~~the more-most~~ exceptional ESL conditions (RP 250 in 2100),
 360 the barrier is ~~surmounted/overtopped~~, generating a flood extent similar to the baseline scenario for the same
 361 occurrence probability.

Formatted: Font: Palatino Linotype, 10 pt, Italic



362

363 **Figure 7.** Cesenatico, extent of land affected by flood according to frequency of occurrence of ESL event up to
 364 2100 for the baseline [left] and the defended scenario [right]. Basemap © Google Maps 2020.

365 In Cesenatico, a barrier designed similarly to *Parco del Mare* could provide significant reduction of flood extents
 366 under most hazard scenarios. Its effectiveness would be greater than in Rimini thanks to the complementary
 367 movable barrier system in use, which seals the port channel allowing to wall off the whole coastal perimeter,
 368 reducing the chance of water ingression in the urban area. In contrast, the erodible winter dune in the baseline
 369 defense scenario can only hold the heavy sea for shorter, less intense ESL events (RP 1–10 years), and becomes
 370 ineffective with more exceptional, long-lasting events; ~~at from 2050 on and 2100~~, the winter dune ~~could be gets~~
 371 surmounted and dismantled by sea waves ~~even for during frequent events (RP 1 year) scenario RP250 years~~
 372 ~~(mid and low left maps).~~

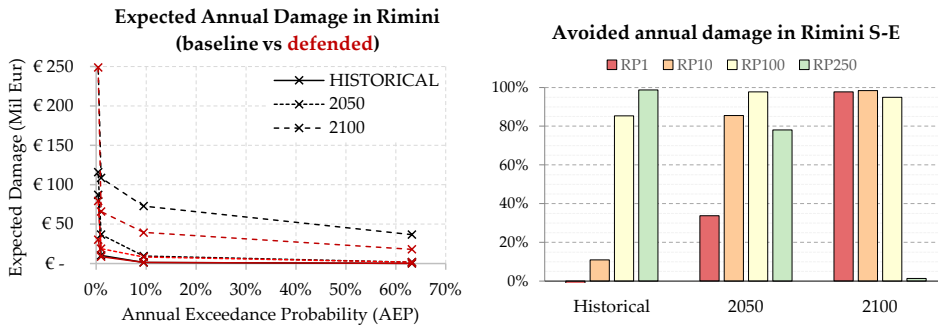
373 4.2 Expected Annual Damage

374 The Expected Annual Damage is calculated as a function of maximum exposed value and water depth. In
 375 Rimini, the EAD grows from around 650 thousand Eur under historical conditions to 2.8 million Eur in 2050

Formatted: Font: Palatino Linotype, 10 pt, Italic, English (United States)

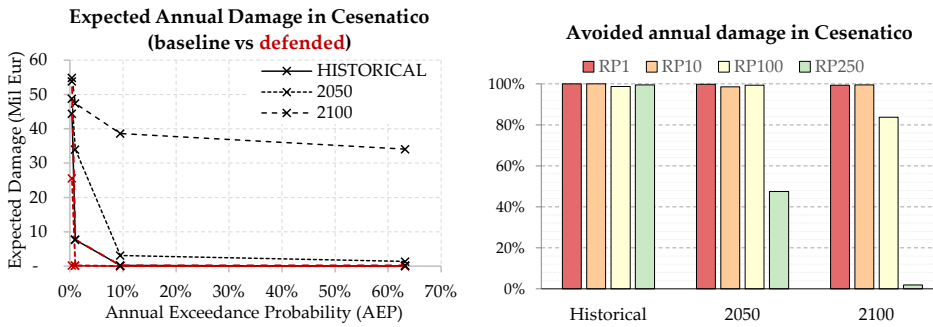
376 and more than 32.3 million Eur in 2100. ~~With~~ Under less severe ~~events~~ ESL scenarios (up to RP below 100
 377 years), the risk remains mostly confined around the marina ~~area, which is located~~ (outside the ~~protection~~
 378 ~~offered by the reinforced dune defended area~~) producing an ~~expected damage EAD~~ below 10 thousand Eur.;
 379 Under with more ~~intense extreme~~ ESL scenarios, (i.e. RP 250 years), the benefits of the ~~dune barrier~~ Parco del
 380 ~~Mare project (i.e. defended scenario)~~, protecting the southern part of Rimini become more evident, avoiding
 381 about 65% of the ~~EAD expected damages in the defended scenarios comparison compared with to the~~
 382 ~~undefended scenarios~~. The damage avoided in the defended ~~area scenarios~~ grows almost linearly with the
 383 increase of ~~the baseline~~ EAD under future projections of sea level rise: under the defended ~~hypothesis scenario~~,
 384 the EAD is reduced on average by 45% ~~in comparison with the undefended scenario~~ (figure 8, left). The project
 385 produces benefit up to ~~ESL scenario~~ RP 250 years in 2100, where a projected TWL of 3.5 meters would cause
 386 the ~~surmounting overtopping~~ of the barrier, reducing the ~~benefits~~ to almost zero (figure 8, right).

Formatted: Font: Palatino Linotype, 10 pt, Italic



387
 388 **Figure 8.** Rimini: Expected Annual Damage (EAD) according to undefended scenario up to 2100, ~~all town~~
 389 ~~considered~~ [left]; EAD reduction in the ~~south-eastern~~ part of the town thanks to hazard mitigation offered
 390 by the coastal barrier [right].

391 In Cesenatico, the average EAD for the undefended scenario grows from around 270 thousand Eur under
 392 historical conditions, to 1.7 million Eur in 2050 and almost 26 million Eur in 2100. In our simulations, the
 393 designed defence structure (a static barrier with height of 2.8 m along 7.8 km of coast) is able to avoid most of
 394 the damage inflicted to residential buildings (figure 9, left). The measure becomes less efficient for the most
 395 extreme scenarios in 2050 and 2100, when the increase in TWL causes the surmounting of the barrier (figure
 396 9, right). This assessment does not account for the ~~impacts over those~~ beach resorts and bathing facilities,
 397 which are located along the barrier or between the barrier and the sea, and thus are equally exposed in both
 398 the baseline and the defended scenario; they would likely represent an additional 7-25% of the baseline
 399 damage.



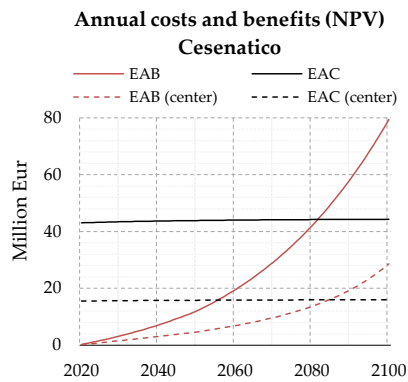
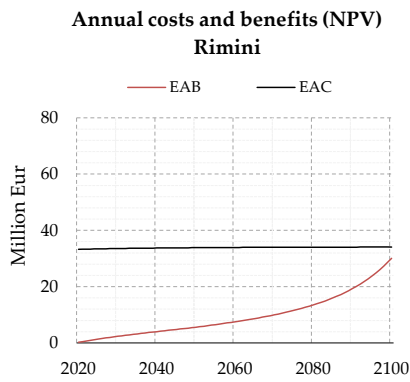
400
 401 **Figure 9.** Cesenatico: Expected Annual Damage (EAD) according to undefended scenario up to 2100 [left];
 402 EAD reduction thanks to hazard mitigation offered by the coastal barrier [right].

403 **4.3 Cost-Benefit Analysis**

404 The estimates of avoided direct flood impacts are accounted in a DRR-oriented CBA to evaluate the feasibility
 405 of mitigation measures in terms of NPV, BCR and payback period for the two time-horizons (2021-2050: 30
 406 years; and 2021-2100: 80 years). The assessment does not measure the indirect benefits brought in terms of
 407 urban renovation, which are the primary focus of the *Parco del Mare* project, measuring, instead, only the direct
 408 benefits in terms of direct flood damage reduction. In figure 10, the Expected Annual Benefits (EAB) grow at
 409 faster rate approaching 2100 in both sites, because of the larger expected damages from more intense, less
 410 frequent flood events. The cost of defence implementation is repaid by avoided damage after about 40 years
 411 in Cesenatico and after 90 years in Rimini. At 2100, the BCR is 0.9 for Rimini and 1.8 for Cesenatico. These
 412 results clearly indicate an overall profitability of the defence structure implementation over the long term for
 413 Cesenatico. For the case of the municipality of Rimini, further investigation is required in order to account for
 414 the non-DRR benefits of the seafront renovation project. For instance, the potential reduction in indirect losses
 415 in terms of capital and labour productivity due to less frequent and less intense flooding events, and the
 416 potential increase in tourism and well-being of citizens due to renewed urban landscape, are factors that could
 417 be accounted for in a holistic CBA analysis and would likely return a shorter payback period.

418 In order to better understand the potential benefits of the mitigation measures over different areas of the two
 419 municipalities, we compare the results in terms of CBR over a selection of exposed records corresponding to
 420 the town higher-density area (i.e. Cesenatico historical center). Table 2 summarizes the metrics of the
 421 assessment for different area extent selections. Results do not differ much when comparing the CBA over
 422 different areas. In Cesenatico benefits grow proportionally to costs, so that the payback time does not change
 423 when considering a section of the town or the whole coastal perimeter.

Formatted: Font: Palatino Linotype, 10 pt, Italic, English (United States)



424

425 **Figure 10.** Cumulated flood defence costs and expected benefits at Net Present Value for Rimini (left) and
 426 Cesenatico (right).

427

428

429 **Table 2.** Summary of CBA for planned or designed seaside defence project in Rimini (all town and south
 430 section only) and Cesenatico (all town and center only) over a time horizon of 30 and 80 years (~~2020-2021~~ to
 431 2050 and ~~2020-2021~~ to 2100).

Metrics	Rimini				Cesenatico			
	All town		South only		All town		Center only	
	2050	2100	2050	2100	2050	2100	2050	2100
Baseline EAD [M EUR]	2.8	32	0.5	14.6	1.7	25.9	0.5	12.4
Defended EAD [M EUR]	2.4	17	0.1	0.9	0.1	0.4	0.1	0.4
Expected Annual Benefits [M EUR]	0.3	15	0.4	13.7	1.6	25.5	0.4	11.9
Sum of EAB (discounted) [M EUR]	5.6	30	4.1	27.8	12.0	79.4	4.7	28.6
Sum of EAC (discounted) [M EUR]	33.8	34.0	33.8	34.0	43.8	44.3	15.8	16.0
Net Present Value [M EUR]	-28.3	-4.0	-29.8	-6.3	-31.8	35.1	-11.24	12.6
Benefit-Cost ratio [-]	0.16	0.88	0.12	0.81	0.28	1.79	0.30	1.79

432 5. Conclusion

433 In this study we addressed coastal inundation risk scenarios over two coastal towns located along the North
 434 Adriatic coastal plain of Italy, which is projected to become increasingly exposed to ESL events due to changes
 435 in MSL induced by SLR and local subsidence phenomena. Both locations are expected to suffer increasing
 436 economic losses from these events, unless effective coastal adaptation measures are put in place. To
 437 understand the upcoming impacts and the potential benefits of designed coastal projects, we run a CBA
 438 comparing the baseline and the defended scenario in terms of flood losses over residential buildings, which
 439 represent the largest share of exposed buildings' footprints (93%). The defended scenario accounts for the
 440 effect of a coastal barriers based on the design of ~~the "Parco del Mare"~~, an urban renovation project under
 441 construction in Rimini. The same type of defence structure is envisaged along the coastal perimeter of the
 442 nearby town of Cesenatico. First, we characterised reference ESL events in terms of frequency and intensity
 443 based on local historical observations; then, we projected ESL scenarios to 2050 and 2100, accounting for the
 444 combined effect of eustatic SLR and subsidence rates on the TWL, as obtained from existing local studies. We
 445 produced flood hazard maps estimating maximum flood extent and water depth using a high-resolution
 446 hydrodynamic model able to replicate the physics of the inundation process. The hazard maps were fed to ~~the~~
 447 a locally-calibrated damage model in order to calculate the expected annual damage for both baseline and
 448 defended scenarios. An increase in damage is expected for both urban areas from ~~2020-2021~~ to 2100: in
 449 Cesenatico the EAD grows by a factor 96, in Rimini by a factor 49.

450 The results obtained from the CBA on both locations show growing profitability of present project investment
 451 over time, associated with the increase of ~~expected annual~~ damage ~~from triggered by~~ intense ESL events: the
 452 EAD under the baseline hypothesis is expected to increase by 3.5-fold in 2050, up to 10-fold in 2100. The
 453 benefits brought by the coastal defence project become much larger in the second half of the century: the EAB
 454 grows 6.1-fold in Rimini, 6.5-fold in Cesenatico, from 2050 to 2100. Avoided losses are expected to match the
 455 project implementation costs after about 40 years in Cesenatico and 90 years in Rimini. Benefits are found to
 456 increase proportionally to costs; the payback period in Cesenatico is the same considering either an investment
 457 on the protection of the whole town or only part of it. Further assessments of these renovation projects should
 458 look to measure the indirect and spill-over effects over the local economy brought by the project, possibly
 459 accounting also for the intangible benefits and scenarios of exposure change. The results are calculated in
 460 relation to emission scenario RCP 4.5; compared to RCP 8.5 at 2050, the difference in SLR contribution is
 461 negligible (~0.05 m), while at 2100, the difference between the two emission scenarios is larger (around 0.2 m),
 462 thus additional scenario analysis is suggested in future research.

Formatted: Font: Palatino Linotype, 10 pt, Italic

463 **Data availability**

464 Mattia Amadio, & Arthur H. Essenfelder. (2021). Coastal flood inundation scenarios over Cesenatico and
465 Rimini: hazard and risk for Business as Usual and Defended options [Data set]. *Natural Hazard and Earth
466 System Sciences Hosted by Zenodo*: <https://zenodo.org/record/4783443><http://doi.org/10.5194/nhess-2020-414>

467 **Authors contribution**

468 MA, AHE and SB conceptualized the study and designed the experiments. AHE carried out the coastal hazard
469 modelling. SR advised the model setup and calculation. SB and PM provided required data and expertise
470 about the case study areas. MA performed the economic risk modelling and wrote the manuscript. SM
471 supported the CBA calculations. JM and SB managed the funding acquisition and project supervision. All co-
472 authors have reviewed the manuscript.

473 **Acknowledgment**

474 The research leading to this paper received funding through the projects CLARA (EU's Horizon 2020 research
475 and innovation programme under grant agreement 730482), SAFERPLACES (Climate-KIC innovation
476 partnership) and EUCP – European Climate Prediction system under grant agreement 776613. We want to
477 thank Luisa Perini for her kind support.

478 **References**

- 479 Amadio M, Scorzini AR, Carisi F, et al (2019) Testing empirical and synthetic flood damage models: the case
480 of Italy. *Nat Hazards Earth Syst Sci* 19:661–678. <https://doi.org/10.5194/nhess-19-661-2019>
- 481 Antonioli F, Anzidei M, Amorosi A, et al (2017) Sea-level rise and potential drowning of the Italian coastal
482 plains: Flooding risk scenarios for 2100. *Quat Sci Rev* 158:29–43.
483 <https://doi.org/10.1016/j.quascirev.2016.12.021>
- 484 Armaroli C, Ciavola P, Perini L, et al (2012) Critical storm thresholds for significant morphological changes
485 and damage along the Emilia-Romagna coastline, Italy. *Geomorphology* 143–144:34–51.
486 <https://doi.org/10.1016/j.geomorph.2011.09.006>
- 487 Armaroli C, Duo E (2018) Validation of the coastal storm risk assessment framework along the Emilia-
488 Romagna coast. *Coast Eng* 134:159–167. <https://doi.org/10.1016/j.coastaleng.2017.08.014>
- 489 ARPAE (2019) *Relazione tecnica mappe della pericolosità e del rischio di alluvioni in ambito costiero*
- 490 Boardman AE, Greenberg DH, Vining AR, Weimer DL (2018) *Cost-Benefit Analysis*. Cambridge University
491 Press
- 492 Bonaduce A, Pinardi N, Oddo P, et al (2016) Sea-level variability in the Mediterranean Sea from altimetry
493 and tide gauges. *Clim Dyn* 47:2851–2866. <https://doi.org/10.1007/s00382-016-3001-2>
- 494 Bos F, Zwaneveld P (2017) *Cost-Benefit Analysis for Flood Risk Management and Water Governance in the
495 Netherlands: An Overview of One Century*. SSRN Electron J. <https://doi.org/10.2139/ssrn.3023983>
- 496 Bouwer LM (2011) Have disaster losses increased due to anthropogenic climate change? *Bull Am Meteorol
497 Soc*. <https://doi.org/10.1175/2010BAMS3092.1>
- 498 Carbognin L, Teatini P, Tomasin A, Tosi L (2010) Global change and relative sea level rise at Venice: What
499 impact in term of flooding. *Clim Dyn* 35:1055–1063. <https://doi.org/10.1007/s00382-009-0617-5>
- 500 Carbognin L, Teatini P, Tosi L (2009) The impact of relative sea level rise on the Northern Adriatic Sea coast,
501 Italy. *WIT Trans Ecol Environ* 127:137–148. <https://doi.org/10.2495/RAV090121>

502 Carminati E, Martinelli G (2002) Subsidence rates in the Po Plain, northern Italy: the relative impact of
503 natural and anthropogenic causation. *Eng Geol* 66:241–255. [https://doi.org/10.1016/S0013-](https://doi.org/10.1016/S0013-7952(02)00031-5)
504 7952(02)00031-5

505 Church JA, White NJ (2011) Sea-Level Rise from the Late 19th to the Early 21st Century. *Surv Geophys*
506 32:585–602. <https://doi.org/10.1007/s10712-011-9119-1>

507 Ciavola P, Coco G (eds) (2017) *Coastal storms: processes and impacts*. Wiley-Blackwell

508 Comune di Rimini (2018) *Parco del Mare Sud - Strategia per la rigenerazione urbana*

509 Comune di Rimini (2019a) *Deliberazione originale di giunta comunale N. 99 del 11/04/2019*

510 Comune di Rimini (2019b) *Deliberazione originale di giunta comunale N. 118 del 02/05/2019*

511 Comune di Rimini (2020) *Deliberazione originale di giunta comunale N. 128 del 26/05/2020*

512 Comune di Rimini (2021a) *Deliberazione originale di giunta comunale N. 19 del 19/01/2021*

513 Comune di Rimini (2021b) *Deliberazione originale di giunta comunale N. 20 del 19/01/2021*

514 CRESME (2014) *Definizione dei costi di (ri)costruzione nell'edilizia*

515 Froehlich DC (2002) *IMPACT Project Field Tests 1 and 2: "Blind" Simulation*. 1–18

516 Gambolati G, Giunta G, Putti M, et al (1998) Coastal Evolution of the Upper Adriatic Sea due to Sea Level
517 Rise and Natural and Anthropic Land Subsidence. 1–34. <https://doi.org/10.1007/978-94-011-5147-4>

518 Garnier E, Ciavola P, Spencer T, et al (2018) Historical analysis of storm events: Case studies in France,
519 England, Portugal and Italy. *Coast Eng* 134:10–23. <https://doi.org/10.1016/j.coastaleng.2017.06.014>

520 Geofabrik GmbH (2018) *OpenStreetMap data extracts*

521 Hallegatte S, Green C, Nicholls RJ, Corfee-Morlot J (2013) Future flood losses in major coastal cities. *Nat*
522 *Clim Chang*. <https://doi.org/10.1038/nclimate1979>

523 Hinkel J, Lincke D, Vafeidis AT, et al (2014) Coastal flood damage and adaptation costs under 21st century
524 sea-level rise. *Proc Natl Acad Sci*. <https://doi.org/10.1073/pnas.1222469111>

525 Huizinga J, Moel H De, Szewczyk W (2017) *Global flood depth-damage functions : Methodology and the*
526 *Database with Guidelines*

527 IPCC (2019) *IPCC Special Report on the Ocean and Cryosphere in a Changing Climate*

528 ISPRA (2012) *Mare e ambiente costiero. Temat Primo Piano - Annu dei dati Ambient 2011* 259–322

529 ISTAT (2011) *15° censimento della popolazione e delle abitazioni*

530 Jongman B, Kreibich H, Apel H, et al (2012a) Comparative flood damage model assessment: towards a
531 European approach. *Nat Hazards Earth Syst Sci* 12:3733–3752

532 Jongman B, Ward PJ, Aerts JCH (2012b) Global exposure to river and coastal flooding: Long term trends
533 and changes. *Glob Environ Chang*. <https://doi.org/10.1016/j.gloenvcha.2012.07.004>

534 Jonkman SN, Brinkhuis-Jak M, Kok M (2004) Cost benefit analysis and flood damage mitigation in the
535 Netherlands. *Heron* 49:95–111

536 Kain CL, Lewarn B, Rigby EH, Mazengarb C (2020) Tsunami Inundation and Maritime Hazard Modelling
537 for a Maximum Credible Tsunami Scenario in Southeast Tasmania, Australia. *Pure Appl Geophys*
538 177:1549–1568. <https://doi.org/10.1007/s00024-019-02384-0>

539 Kemp AC, Horton BP, Donnelly JP, et al (2011) Climate related sea-level variations over the past two
540 millennia. *Proc Natl Acad Sci U S A* 108:11017–11022. <https://doi.org/10.1073/pnas.1015619108>

541 Kind JM (2014) Economically efficient flood protection standards for the Netherlands. *J Flood Risk Manag*
542 7:103–117. <https://doi.org/10.1111/jfr3.12026>

- 543 Kirezci E, Young IR, Ranasinghe R, et al (2020) Projections of global-scale extreme sea levels and resulting
544 episodic coastal flooding over the 21st Century. *Sci Rep* 10:1–12. <https://doi.org/10.1038/s41598-020-67736-6>
545
- 546 Lambeck K, Antonioli F, Anzidei M, et al (2011) Sea level change along the Italian coast during the Holocene
547 and projections for the future. *Quat Int* 232:250–257. <https://doi.org/10.1016/j.quaint.2010.04.026>
- 548 Lambeck K, Purcell A (2005) Sea-level change in the Mediterranean Sea since the LGM: Model predictions
549 for tectonically stable areas. In: *Quaternary Science Reviews*. Pergamon, pp 1969–1988
- 550 Lionello P (2012) The climate of the Venetian and North Adriatic region: Variability, trends and future
551 change. *Phys Chem Earth* 40–41:1–8. <https://doi.org/10.1016/j.pce.2012.02.002>
- 552 Lionello P, Barriopedro D, Ferrarin C, et al (2020) Extremes floods of Venice: characteristics, dynamics, past
553 and future evolution. *Nat Hazards Earth Syst Sci* 1–34. <https://doi.org/10.5194/nhess-2020-359>
- 554 Lowe J (2008) Intergenerational wealth transfers and social discounting: Supplementary Green Book
555 guidance. HM Treasury, London 3–6
- 556 Lowe J, Gregory J, Flather R (2001) Changes in the occurrence of storm surges around the United Kingdom
557 under a future climate scenario using a dynamic storm surge model driven by the Hadley Centre
558 climate models. *Clim Dyn* 18:179–188
- 559 Marsico A, Lisco S, Lo Presti V, et al (2017) Flooding scenario for four Italian coastal plains using three
560 relative sea level rise models. *J Maps* 13:961–967. <https://doi.org/10.1080/17445647.2017.1415989>
- 561 Masina M, Lamberti A, Archetti R (2015) Coastal flooding: A copula based approach for estimating the joint
562 probability of water levels and waves. *Coast Eng* 97:37–52.
563 <https://doi.org/10.1016/j.coastaleng.2014.12.010>
- 564 McGranahan G, Balk D, Anderson B (2007) The rising tide: Assessing the risks of climate change and human
565 settlements in low elevation coastal zones. *Environ Urban*. <https://doi.org/10.1177/0956247807076960>
- 566 McInnes KL, Walsh KJE, Hubbert GD, Beer T (2003) Impact of sea-level rise and storm surges in a coastal
567 community. *Nat Hazards* 30:187–207. <https://doi.org/10.1023/A:1026118417752>
- 568 Mechler R (2016) Reviewing estimates of the economic efficiency of disaster risk management: opportunities
569 and limitations of using risk-based cost–benefit analysis. *Nat Hazards* 81:2121–2147.
570 <https://doi.org/10.1007/s11069-016-2170-y>
- 571 Meli M, Olivieri M, Romagnoli C (2021) Sea-level change along the emilia-romagna coast from tide gauge
572 and satellite altimetry. *Remote Sens* 13:1–26. <https://doi.org/10.3390/rs13010097>
- 573 Meyssignac B, Cazenave A (2012) Sea level: A review of present-day and recent-past changes and variability.
574 *J. Geodyn*. 58:96–109
- 575 Mitchum GT, Nerem RS, Merrifield MA, Gehrels WR (2010) Modern Sea-Level-Change Estimates. In:
576 *Understanding Sea-Level Rise and Variability*. Wiley-Blackwell, Oxford, UK, pp 122–142
- 577 Muis S, Verlaan M, Winsemius HC, et al (2016) A global reanalysis of storm surges and extreme sea levels.
578 *Nat Commun* 7:1–11. <https://doi.org/10.1038/ncomms11969>
- 579 Nicholls RJ, Cazenave A (2010) Sea-level rise and its impact on coastal zones. *Science* (80-) 328:1517–1520.
580 <https://doi.org/10.1126/science.1185782>
- 581 Olsen AS, Zhou Q, Linde JJ, Arnbjerg-Nielsen K (2015) Comparing methods of calculating expected annual
582 damage in urban pluvial flood risk assessments. *Water* (Switzerland) 7:255–270.
583 <https://doi.org/10.3390/w7010255>
- 584 Peltier WR (2004) Global Glacial Isostasy and the surface of the ice-age Earth: the ICE-5G (VM2) Model and
585 GRACE. *Annu Rev Earth Planet Sci* 32:111–149. <https://doi.org/10.1146/annurev.earth.32.082503.144359>

- 586 Peltier WR, Argus DF, Drummond R (2015) Space geodesy constrains ice age terminal deglaciation: The
587 global ICE-6G_C (VM5a) model. *J Geophys Res Solid Earth* 120:450–487.
588 <https://doi.org/10.1002/2014JB011176>
- 589 Perini L, Calabrese L, Deserti M, et al (2011) Le mareggiate e gli impatti sulla costa in Emilia-Romagna 1946-
590 2010
- 591 Perini L, Calabrese L, Lorito S, Luciani P (2015) Il rischio da mareggiata in Emilia-Romagna: l'evento del 5-6
592 Febbraio 2015. *Geol* 53:8–17
- 593 Perini L, Calabrese L, Luciani P, et al (2017) Sea-level rise along the Emilia-Romagna coast (Northern Italy) in
594 2100: Scenarios and impacts. *Nat Hazards Earth Syst Sci* 17:2271–2287. <https://doi.org/10.5194/nhess-17-2271-2017>
595
- 596 Perini L, Calabrese L, Salerno G, et al (2016) Evaluation of coastal vulnerability to flooding: Comparison of
597 two different methodologies adopted by the Emilia-Romagna region (Italy). *Nat Hazards Earth Syst Sci*
598 16:181–194. <https://doi.org/10.5194/nhess-16-181-2016>
- 599 Perini L, Calabrese L, Salerno G, Luciani P (2012) Mapping of flood risk in Emilia-Romagna coastal areas.
600 *Rend Online Soc Geol Ital* 21:501–502. <https://doi.org/10.13140/2.1.1703.7766>
- 601 Polcari M, Albano M, Montuori A, et al (2018) InSAR monitoring of Italian coastline revealing natural and
602 anthropogenic ground deformation phenomena and future perspectives. *Sustain* 10:4–7.
603 <https://doi.org/10.3390/su10093152>
- 604 Price R (2018) Cost-effectiveness of disaster risk reduction and adaptation to climate change. 1–21
- 605 Roberts S (2020) ANUGA - Open source hydrodynamic / hydraulic modelling
- 606 Roberts S, Nielsen O, Gray D, Sexton J (2015) ANUGA User Manual
- 607 Solari L, Del Soldato M, Bianchini S, et al (2018) From ERS 1/2 to Sentinel-1: Subsidence Monitoring in Italy
608 in the Last Two Decades. *Front Earth Sci* 6:. <https://doi.org/10.3389/feart.2018.00149>
- 609 Stocker TF, Dahe Q, Plattner G-K, et al (2013) Technical Summary. In: Stocker TF, Qin D, Plattner G-K, et al.
610 (eds) *Climate Change 2013: The Physical Science Basis. Contribution of Working Group I to the Fifth*
611 *Assessment Report of the Intergovernmental Panel on Climate Change*. Cambridge University Press,
612 Cambridge, United Kingdom and New York, NY, USA., pp 33–115
- 613 Syvitski JPM, Kettner AJ, Overeem I, et al (2009) Sinking deltas due to human activities. *Nat Geosci*.
614 <https://doi.org/10.1038/ngeo629>
- 615 Teatini P, Ferronato M, Gambolati G, et al (2005) A century of land subsidence in Ravenna, Italy. *Environ*
616 *Geol* 47:831–846. <https://doi.org/10.1007/s00254-004-1215-9>
- 617 Teatini P, Ferronato M, Gambolati G, Gonella M (2006) Groundwater pumping and land subsidence in the
618 Emilia-Romagna coastland, Italy: Modeling the past occurrence and the future trend. *Water Resour Res*
619 42:. <https://doi.org/10.1029/2005WR004242>
- 620 Tsimplis MN, Raicich F, Fenoglio-Marc L, et al (2012) Recent developments in understanding sea level rise at
621 the Adriatic coasts. *Phys Chem Earth* 40–41:59–71. <https://doi.org/10.1016/j.pce.2009.11.007>
- 622 Tsimplis MN, Rixen M (2002) Sea level in the Mediterranean Sea: The contribution of temperature and
623 salinity changes. *Geophys Res Lett* 29:51-1-51-4. <https://doi.org/10.1029/2002gl015870>
- 624 Umgiesser G, Bajo M, Ferrarin C, et al (2020) The prediction of floods in Venice: methods, models and
625 uncertainty. *Nat Hazards Earth Syst Sci* 1–47. <https://doi.org/10.5194/nhess-2020-361>
- 626 Vousdoukas MI, Mentaschi L, Feyen L, Voukouvalas E (2017) Extreme sea levels on the rise along Europe's
627 coasts. *Earth's Futur* 5:1–20. <https://doi.org/10.1002/eff2.192>
- 628 Vousdoukas MI, Mentaschi L, Voukouvalas E, et al (2018) Global probabilistic projections of extreme sea

Formatted: German (Germany)

629 levels show intensification of coastal flood hazard. Nat Commun 9:1–12. [https://doi.org/10.1038/s41467-](https://doi.org/10.1038/s41467-018-04692-w)
 630 018-04692-w

631 Wöppelmann G, Marcos M (2012) Coastal sea level rise in southern Europe and the nonclimate contribution
 632 of vertical land motion. J Geophys Res Ocean 117:. <https://doi.org/10.1029/2011JC007469>

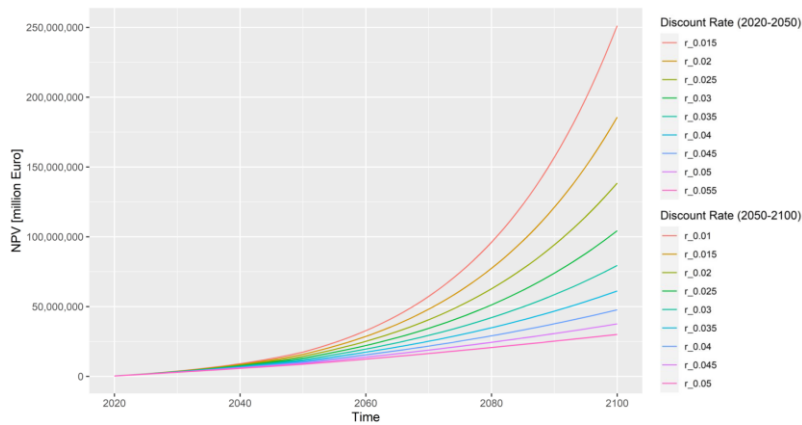
633 Zanchettin D, Bruni S, Raicich F, et al (2020) Review article: Sea-level rise in Venice: historic and future
 634 trends. Nat Hazards Earth Syst Sci Discuss 1–56. <https://doi.org/10.5194/nhess-2020-351>

635 Zanchettin D, Traverso P, Tomasino M (2007) Observations on future sea level changes in the Venice lagoon.
 636 Hydrobiologia. <https://doi.org/10.1007/s10750-006-0416-5>

637

638 **Annex 1**

639 A sensitivity analysis is carried out on the discount rate. Figure A1 below shows how the NPV changes with
 640 discount rate r ranging from 1.5% to 5.5% (2020 to 2050) and 1% to 5% (2050–2100).



641
 642

Figure A1. Sensitivity analysis of NPV using a variable discount rate.